Characterization of Biodegradable Polymers by Inverse Gas Chromatography. II. Blends of Amylopectin and Poly(ε-caprolactone)

Ali Al-Ghamdi,* Mohammad Melibari,[1,†] Zeki Y. Al-Saigh

Department of Chemistry, State University of New York, Buffalo State College, 1300 Elmwood Avenue, Buffalo, New York 14222

Received 6 October 2005; accepted 30 January 2006
DOI 10.1002/app.24226
Published online in Wiley InterScience (www.interscience.wiley.com).

ABSTRACT: Amylopectin (AP), a potato-starch-based polymer with a molecular weight of 6,000,000 g/mol, was blended with poly(ε-caprolactone) (PCL) and characterized with inverse gas chromatography (IGC), differential scanning calorimetry (DSC), and X-ray diffraction (XRD). Five different compositions of AP–PCL blends ranging from 0 to 100% AP were studied over a wide range of temperatures (80–260°C). Nineteen solutes (solvents) were injected onto five chromatographic columns containing the AP–PCL blends. These solutes probed the dispersive, dipole–dipole, and hydrogen-bonding interactions, acid–base characteristics, wettability, and water uptake of the AP–PCL blends. Retention diagrams of these solutes in a temperature range of 80–260°C revealed two zones: crystalline and amorphous. The glass-transition temperature (T_g) and melting temperature (T_m) of the blends were measured with these zones. The two zones were used to calculate the degree of crystallinity of pure AP and its blends below T_m, which ranged from 85% at 104°C to 0% at T_m. IGC complemented the DSC method for obtaining the T_g and T_m values of the pure AP and AP–PCL blends. These values were unexpectedly elevated for the blends over that of pure AP and ranged from 105 to 152°C for T_g and from 166 to 210°C for T_m. The T_m values agreed well with the XRD analysis data. This elevation in the T_g and T_m values may have been due to the change in the heat capacity at T_g and the dependence of T_g on various variables, including the molecular weight and the blend composition. Polymer blend/solvent interaction parameters were measured with a variety of solutes over a wide range of temperatures and determined the solubility of the blends in the solutes. We were also able to determine the blend compatibility over a wide range of temperatures and weight fractions. The polymer–polymer interaction coefficient and interaction energy parameter agreed well on the partial miscibility of the two polymers. The dispersive component of the surface energy of the AP–PCL blends was measured with alkanes and ranged from 16.09 mJ/m^2 for pure AP to 38.26 mJ/m^2 when AP was mixed with PCL in a 50/50% ratio. This revealed an increase in the surface energy of AP when PCL was added. J Appl Polym Sci 101: 3076–3089, 2006

Key words: differential scanning calorimetry (DSC); mixing; X-ray

INTRODUCTION

Starch-based materials have been extensively investigated,[1–4] particularly for use as packaging materials, because of the advantage of being renewable sources of polymeric materials. Several methods have been used for the characterization of these materials, such as differential scanning calorimetry (DSC), Fourier transform infrared spectroscopy, scanning electron microscopy, solvent extraction, X-ray diffraction (XRD), optical rotation, nuclear magnetic resonance, polarizing optical microscopy,[5–8] and inverse gas chromatography (IGC).[9] The main sources for the commercial production of starch are potatoes, wheat, corn, and rice. Starch has two polymeric components, amylase and amylopectin (AP); they are built of *z*-D-glacopyranose residues but differ in both structure and function.[9] AP constitutes the greater part (75%) of the starch molecule. The physical characteristics of packaging polymers are greatly influenced by the chemical structure, molecular weight, crystallinity, and processing conditions of the polymers used. It has recently been shown that native starch can be transformed into thermoplastic, resinlike products under destruction and plasticization conditions.[10,11] Other attempts have been made to modify the starch structure to reduce the hydrophilic character of the chain.[12]

Blending two biodegradable polymers is a cost-effective method. The rate of biodegradation is correlated with the type of morphology, crystallinity, surface area, and additives. To accomplish this goal, the physical properties of the blends need to be investigated with a certain precision. Such properties will

**Present address:* King Abdulaziz Military Academy, P. O. Box 73040, Riyadh 11538, Saudi Arabia.
†*Present address:* P. O. Box 34600, Jeddah, Saudi Arabia.
Correspondence to: Z. Y. Al-Saigh (alsaigzy@buffalostate.edu).

provide information on whether the blends are compatible, partially compatible, or noncompatible over a range of temperatures and compositions. IGC is a molecular probe technique used for the characterization of surface and bulk properties of solid materials. Being the reverse of a conventional gas chromatography experiment, a chromatographic column is uniformly packed with the solid material of interest, typically a powder, fiber, or film, to form what is called the *stationary phase*. The stationary phase contains the blend of interest to be examined by IGC. IGC has proved to be a powerful tool for the characterization of solid surfaces such as fibers and powders, particularly those that cannot be easily studied by other methods.[13–26]

IGC has been applied to several studies of natural polymers, including cellulose[27] and wood,[28] with respect to the surface energy, surface acid–base free energy, enthalpy of desorption of acid–base probes, surface acid–base acceptors and donor parameters,[28] and lignocellosic surfaces.[29] In this work, we studied the properties of starch (AP) by blending AP with a biodegradable polymer, poly(ε-caprolactone) (PCL). Blends of AP as a resinlike thermoplastic with PCL have been attempted in recent years, and the properties of the resulting blends have been studied with techniques other than IGC.[11] It has been reported that the blending process results in inferior mechanical properties, and the biodegradability of the blends is increased.[30] Averous et al.[31] observed a significant improvement in the properties of blends due to the presence of PCL, which decreased the material modulus but improved the impact resistance. Special attention was devoted to the surface, mechanical, and chemical properties of the new blends. In our experiments, attempts were made to understand the physicochemical properties, and this could lead to the development of methods for determining the water sensitivities and degradation rates of starch-based blends. We found that the IGC method was able to yield information on the thermodynamic, surface, crystallinity, and thermal properties of the AP–PCL blends.

THERMODYNAMICS OF IGC

A complete analysis of the thermodynamics of IGC was recently reviewed.[26] Thermodynamic quantities can be easily obtained from the chromatographic quantities in IGC experiments by the measurement of the specific retention volume (V_g^0). The following equation is used in this study:

$$V_g^0 = \frac{273.15\ \Delta t F J}{w T_r} \quad (1)$$

where $\Delta t = t_p - t_m$ is the difference between the retention times of the solute (t_p) and the marker (t_m). Air is usually used as a marker, when the thermal conductivity detector is used, to account for the dead volume in the chromatographic column. t_m has to be subtracted from t_p to reflect the absolute value of t_p as Δt. F is the flow rate of the carrier gas measured at room temperature (T_r), w is the mass of the stationary phase, and J is a pressure gradient correction factor that depends on the inlet and outlet pressures (P_i and P_o, respectively). P_i and P_o are measured with electronic transducers, which are interfaced at the inlet and outlet of the column. These transducers are usually calibrated with a mercury manometer.

To calculate the interaction parameter of the starch–solute system (χ_{12}), V_g^0 from eq. (1) is used as follows:

$$\chi_{12} = \ln\frac{273.15R\nu_2}{V_g^0 V_1 P_1^0} - 1 + \frac{V_1}{M_2\nu_2} - \frac{B_{11} - V_1}{RT}P_1^0 \quad (2)$$

where 1 denotes the solute and 2 denotes the polymer, ν_2 is the specific volume of the polymer at column temperature T, M_1 is the molecular weight of the solute, P_1^0 is the saturated vapor pressure of the solute, V_1 is the molar volume of the solute, R is the gas constant, and B_{11} is the second virial coefficient of the solute in the gaseous state. Equation (2) is used routinely for the calculation of χ_{12} from IGC experiments.

When a polymer blend system is under study, the key term in the miscibility of a polymer–polymer pair is the free energy of mixing (ΔG_m):

$$\Delta G_m = \Delta H_m - T\Delta S_m \quad (3)$$

where ΔS_m is the combinatorial entropy of mixing and ΔH_m is the molar heat of mixing. Flory[32] attributed ΔS_m to the mixing of the segments on a lattice of a fixed volume. Because the entropy depends on the volume, an additional contribution to the entropy of mixing may be necessary in eq. (3). Sanchez[33] developed a theory to allow for this effect by considering that all mixtures obey the equation of state when appropriate reducing parameters, such as the pressure and temperature, are used for the volume. Other equation-of-state theories of mixtures yield ΔS_m values similar to those of Flory. However, the combinatorial entropy becomes negligible as the molecular weight of the polymer becomes high. Therefore, for high-molecular-weight polymers, only the value of ΔH_m describes the miscibility of the polymer pairs. Flory and Huggins first introduced the volume fraction term ϕ_i in their theory, which described polymer solutions with reasonable success.[32] ΔG_m, as described by the Flory–Huggins theory, is

$$\Delta G_{\text{mix}} = RT\{n_1 \ln \varphi_1 + n_2 \ln\varphi_2 + n_1\varphi_2\chi_{12}\} \quad (4)$$

where n_i is the number of moles of the ith component, RT has its usual meaning, and χ_{12} is a parameter that

is inversely proportional to the absolute temperature. χ_{12} is the same parameter introduced in eq. (2), in which it is an enthalpic contact parameter. The two logarithmic terms represent the (combinatorial) entropy of mixing. Although the sign of the combinatorial entropy always favors mixing, it is clear that its magnitude is greatly diminished as molar volumes become very large. Thus, at high molecular weights, only a negative polymer–polymer interaction coefficient (χ_{23}) satisfies the condition for the miscibility of a polymer blend.

With V_g^0 calculated from eq. (1), χ_{23} can be derived from ΔG_m [eq. (5)]. When a polymer pair is used as a stationary (liquid) phase in a chromatographic column, subscripts 2 and 3 are used to represent polymers 2 and 3, respectively. Subscript 1 refers to the test solute. The interaction between the two polymers is expressed in terms of ΔG_m. ΔG_m has the same form as eq. (3), except that the subscripts change to 2 and 3. The first two (entropic) terms in this equation are negligible for polymer blends. Thus, for a polymer blend to be miscible (ΔG_m being negative), χ_{23} must be negative. When we consider IGC of polymer blends, ΔG_m must be written for a three-component system. It is usually expressed as follows:

$$\Delta G_{\text{mix}} = RT[n_1 \ln\phi_1 + n_2 \ln\phi_2 + n_3 \ln\phi_3 + n_1\phi_2\chi_{12} + n_1\phi_3\chi_{13} + n_2\phi_3\chi_{23}] \quad (5)$$

When a polymer blend is used as a stationary phase in a chromatographic column, the interaction between the two polymers is expressed in terms of χ_{23} [eq. (6)] as an indicator of the miscibility of the polymer blend. If χ_{23} is negative, then the polymer pair is miscible. Recognizing that for a polymer blend containing polymer 2 and polymer 3, ν_2 in eq. (2) should be replaced by $w_2\nu_2 + w_3\nu_3$, where w_2 and w_3 are the weight fractions and ν_2 and ν_3 are the specific volumes of the two polymers in the blend, we can derive χ_{23} from

$$\chi_{23} = \frac{\ln\dfrac{V^0_{g,\text{blend}}}{W_2\nu_2 + W_3\nu_3} - \phi_2 \ln\dfrac{V^0_{g,2}}{\nu_2} - \phi_3 \ln\dfrac{V^0_{g,3}}{\nu_3}}{\phi_2\phi_3} \quad (6)$$

where W_2 and W_3 are the weight fractions of polymer 2 and 3 and ϕ_2 and ϕ_3 are the volume fractions of the two polymers in the blend. To obtain χ_{23} for a polymer blend, with IGC, χ_{12} and χ_{13} have to be known. Three columns are usually prepared: two from the homopolymers and the third from a blend of the two samples used for the homopolymer columns. A further three columns containing different compositions of the blend can also be prepared if the effect of the weight fraction of the blend on miscibility needs to be explored. These columns were studied under identical conditions of the column temperature, carrier gas flow rate, and inlet pressure of the carrier gas and with the same solutes.

With V_g^0 calculated in eq. (1), the enthalpy of adsorption (ΔH_1^s) of the solute vapor into the polymer blend layer can be calculated as follows:

$$\Delta H_1^s = -R\frac{d \ln V_g^0}{d\dfrac{1}{T}} \quad (7)$$

Recently, a complete theoretical treatment for the calculation of the dispersive component of the surface energy of polymers with alkanes was published elsewhere.[34,35] V_g^0 is related to equilibrium constant K between the adsorbed solute and the polymer surface and ΔG_1^s as follows:

$$\Delta G_1^s = -RT \ln V_g^0 + C \quad (8)$$

Equation (4) relates the energy of adsorption to the surface energy as follows:

$$RT \ln V_g^0 + C = 2Na\sqrt{\gamma_s^d\gamma_i^d} \quad (9)$$

where C is the constant, N is Avogadro's number, a is the cross-sectional area and γ_s^d and γ_i^d are the dispersive components of the solid surface and interactive solute phase, respectively. Equation (4) can be rewritten to yield γ_s^d as follows:

$$\gamma s^{\text{d}} = \left[\frac{1}{4\gamma_{\text{CH}_2}}\right]\left[\frac{(\Delta G_a^{\text{CH2}})^2}{(Na_{CH_2})^2}\right] \quad (10)$$

where γ_{CH_2} is the surface energy of a hydrocarbon consisting only of n-alkanes, a_{CH_2} is the area of one —CH_2— group, and ΔG_a^{CH2} is the free energy of desorption of a CH_2 group. Equation (5) usually tests the IGC method for obtaining γ_s^d of polymers.

EXPERIMENTAL

Materials

AP was purchased from Sigma (St. Louis, MO) with a molecular weight of 6.60×10^6 g/mol as a potato starch. It contained 25% amylase. PCL was purchased from Aldrich (St. Louis, MO) with a molecular weight of 80,000 g/mol. A series of chemically different families of solutes, alkanes, acetates, and alcohols in addition to formic acid, diethyl amine, and water were selected as solutes to interact with the AP–PCL blend. Vanishingly small amounts (0.20 μL) of a series of the selected solutes were injected into the chromatographic column. These solutes probed the dispersive, dipole, hydrogen-bonding, and acid–base interactions as well as the wettability of the starch. A total of 19 solutes (chromatographic-

TABLE I
Chromatographic Column Description

Type	Weight of AP (g)	Weight of PCL (g)	Weight of support (g)	Loading (%)
100% AP	0.4870	0.00	7.921	7
100% PCL	0.00	0.4680	7.921	7
25/75% AP–PCL	0.1250	0.375	7.921	7
50/50% AP–PCL	0.2490	0.2500	7.921	7
75/25% AP–PCL	0.3698	0.1259	7.921	7

grade) were purchased from Aldrich (high-performance-liquid-chromatography-grade). Their purity was checked by gas chromatography before use. A chromatographic support, Chromosorb W (acid-washed and dimethyldichlorosilane treated, 60/80 mesh), was obtained from Analabs (Bridgeport, NJ). Chromatographic columns were made in the laboratory from 5-ft-long copper tubing (1/4-in. o.d.). All copper columns were washed with methanol and annealed for several hours before use. Five chromatographic columns were prepared from five solutions containing different weight fractions of the blend. Each solution was prepared by the dissolution of a certain amount of AP and PCL in hot water and deposited onto 6.953 g of Chromosorb W with a soaking method developed by us earlier.[25] The resulting load of AP–PCL on the column was maintained at 7% to ensure column porosity. Full descriptions of these columns are illustrated in Table I. All columns were studied under identical conditions of the temperature, flow rate, and inlet and outlet pressure of the carrier gas.

Instrumentation and procedure

A complete description of the instrumental setup was outlined earlier.[9] Chromatographic measurements were made with two IGC stations, which consisted of a modified Hewlett–Packard model 5890 gas chromatograph and a Varian model 3800 (Palo Alto, CA). Both chromatographs were equipped with a thermal conductivity detector. The chromatographs were modified to minimize the instrumental artifacts in the measurement of the chromatographic quantities, such as the carrier gas flow rate,[36] inlet and outlet pressures, and column temperature.[25] The chromatographic modifications were extended to include a completely automated data handling system from the injection of the solutes to the final thermodynamic data reports. The Hewlett–Packard 5890 gas chromatograph was equipped with an instrument network to allow communication between the integrator and the computer. The Varian 3800 was fully automated and controlled by STAR software. Data handling and analysis of both chromatographs were made possible by special home-customized programs created to enable a variety of thermodynamic calculations used by the IGC method. These programs used ASCII files of reports as input data for further calculations and analyses. Every report contained elution peak information along with the number of peaks, retention time of every peak, and peak width and height.

Our setup allowed for precise measurements of the retention times of the solutes injected into the chromatographic column. The retention volumes of the solutes on a zero loading column (support only) were stored in a separate file and interpolated over a wide range of temperatures. These retention volumes were then subtracted from those measured on loaded columns. This procedure was used to correct for the effect of the inert solid support on the retention volumes. This automated system was fast and ideal for routine IGC measurements.

RESULTS AND DISCUSSION

Thermal analysis

Recently, we reported the thermal analysis of AP with a molecular weight of 6×10^6 g/mol with DSC and thermogravimetric analysis methods.[9] These analyses were carried out by the U.S. Department of Agriculture Forest Service (Madison, WI). The polymer was decomposed at approximately 343°C with approximately 80% weight loss. The polymer showed two transitions at approximately 105°C accompanied by 6% weight loss and at approximately 166°C with no measurable weight loss. These transitions were also detected by IGC and identified as the glass-transition temperature (T_g) and melting temperature (T_m). Retention diagrams (isotherms) were generated for pure AP by the plotting of $\ln V_g^0$ versus $1/T$ with 19 solutes injected into a chromatographic column. Three chemically different families of solutes, alkanes, acetates, and alcohols showed that the morphology of pure AP had a minimum of two regions: crystalline and amorphous. A third region was identified above 235°C as the depolymerization zone, in which the polymer started to decompose. IGC revealed that pure AP had a T_g of 105°C and a T_m of 160°C, in agreement with the DSC method.

IGC retention diagrams

IGC experiments were performed on five chromatographic columns containing different weight fractions

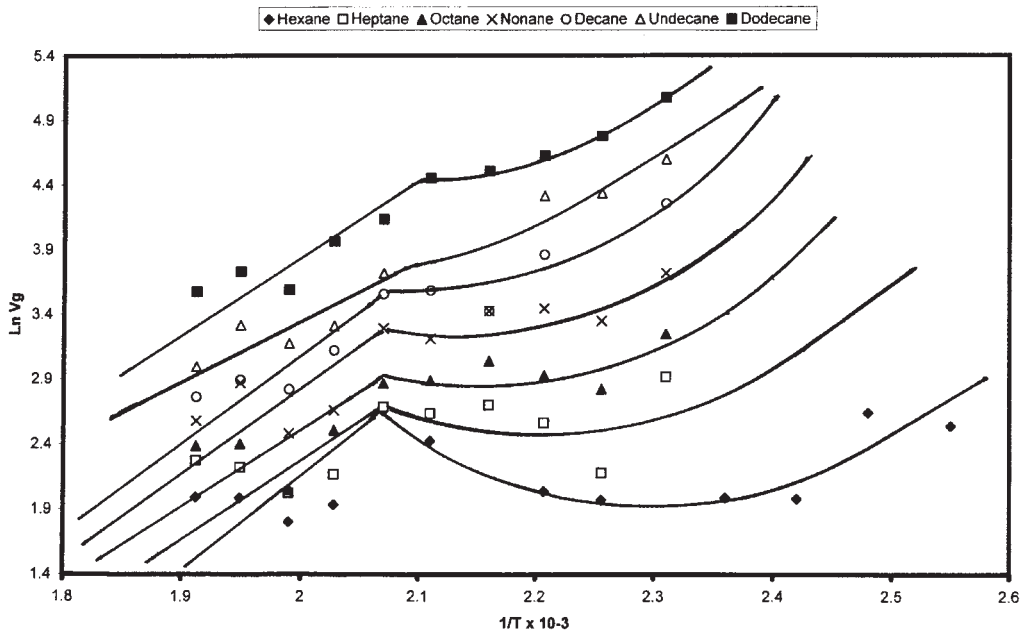

Figure 1 Retention diagram: a blend of the 25/75% AP–alkane system at 80–250°C.

(0–100 wt % AP) of the AP–PCL blends. Nineteen solutes, including series of alkanes, acetates, and alcohols, diethyl amine, formic acid, and water, were injected onto these five columns. With eq. (1), the V_g^0 values of all the solutes were calculated from the chromatographic retention times of these solutes. With eq. (7), a plot of ln V_g^0 versus $1/T$ generates a retention diagram of the blend. Such a diagram reveals the morphology of the blend over a range of temperatures, determines both T_g and T_m, and identifies the thermodynamically valid region above the melt. Figures 1–7 shows the retention diagrams of three AP–PCL blends with weight fractions of 25/75%, 50/50%, and 75/25% AP–PCL. Similar to what we found earlier with AP,[9] two regions could be identified: crystalline and amorphous. IGC experiments were extended beyond the melting of the blend up to 250°C. For some solutes, such as acetates (Fig. 5), a third region could be identified, starting at 203°C because of the thermal depolymerization of the blend.

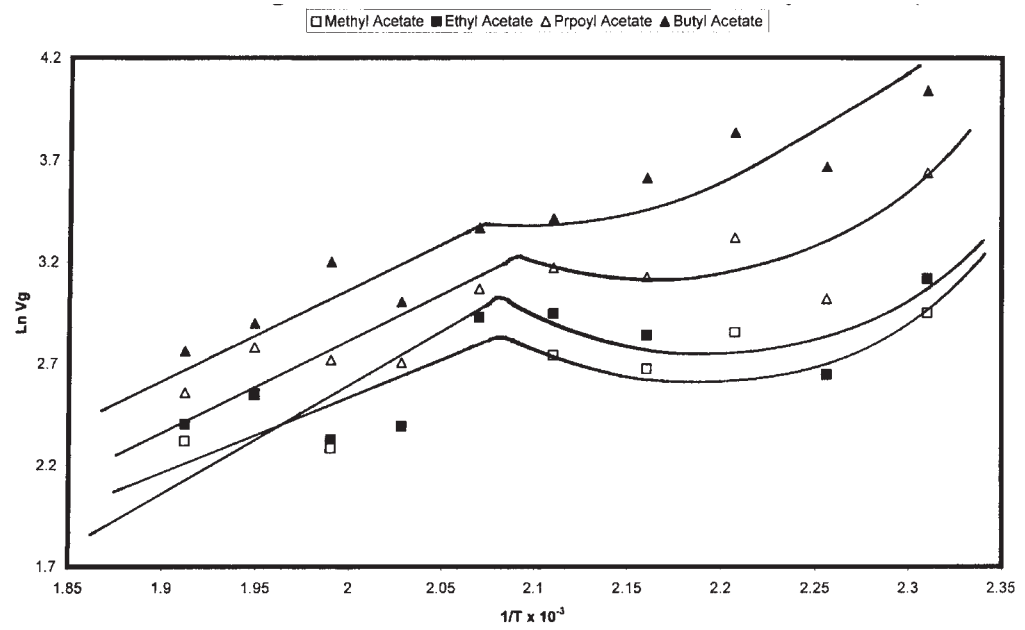

Figure 2 Retention diagram: a blend of the 25/75% AP–acetate system at 80–160°C.

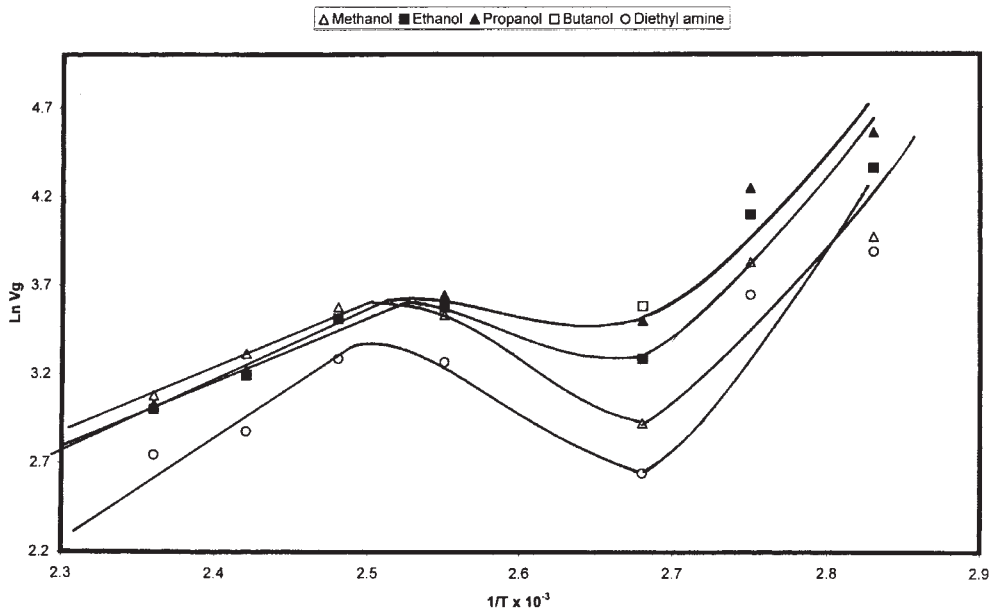

Figure 3 Retention diagram: a blend of the 25/75% AP–alcohol system at 80–160°C.

Some of the retention diagrams involving alcohols as solutes were not complete because of the strong interaction of the alcohols with the blends. The positions of T_g and T_m were unexpectedly higher than those of pure AP. No depression in T_g or T_m was detected. Although T_g was not clearly recognized because of the shallow curvature, the minimum of the curve could be considered T_g of the blend. However, in three retention diagrams (Figs. 3–5), T_g was recognized clearly and measured with more accuracy than in the other diagrams. T_g values ranged from 152°C for 25/75% AP–PCL to 148°C for 50/50% AP–PCL to 120°C for 75/25% AP–PCL. T_m values ranged from 210°C for 25/75% AP–PCL to 181°C for 50/50% AP–PCL to 185°C for 75/25% AP–PCL. The T_m values agreed well with the XRD analysis data (shown later in Fig. 10). The T_m values were consistent among all the retention diagrams and clearly recognizable because of the sharp change in the isotherms. These values were unexpectedly high in comparison with those of pure AP. The blend behavior can be explained by the Gibbs–DiMarzio theory, which offers predictions in-

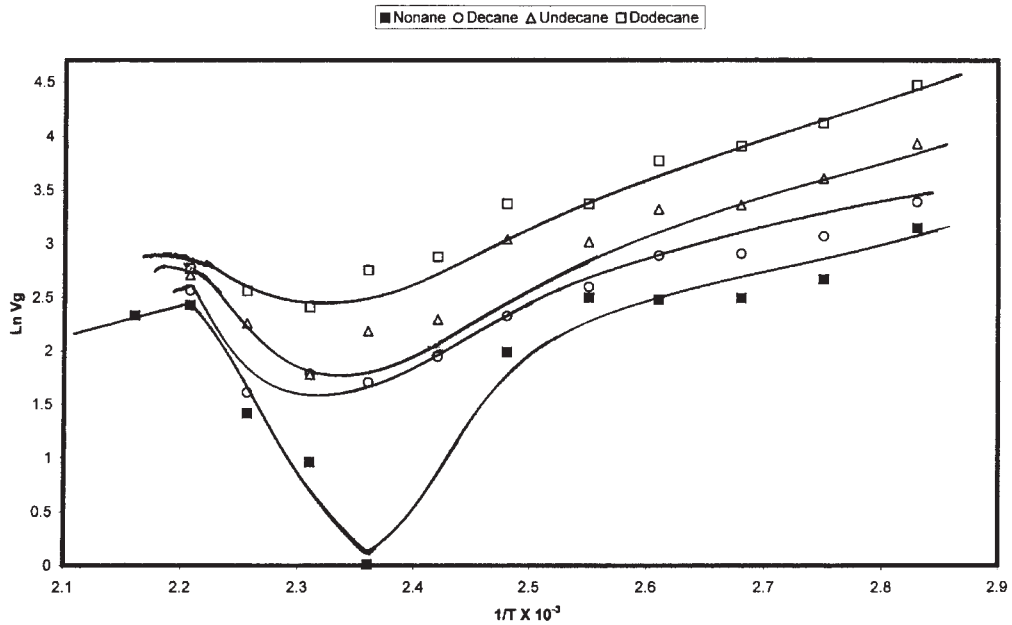

Figure 4 Retention diagram: a blend of the 50/50% AP–alkane system at 80–250°C.

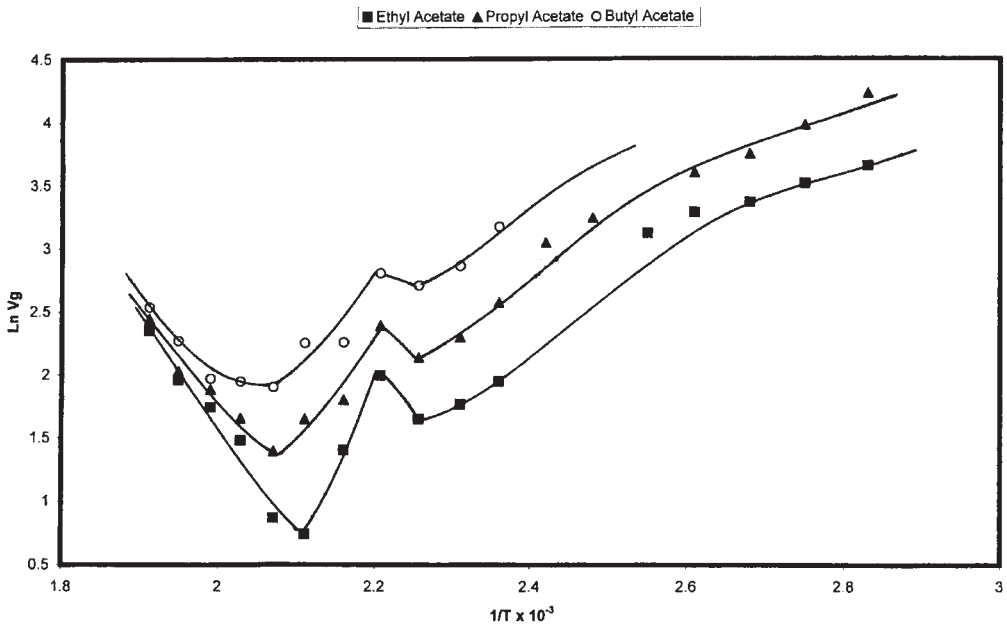

Figure 5 Retention diagram: a blend of the 50/50% AP–acetate system at 80–260°C.

cluding the change in the heat capacity at T_g and the dependence of T_g on various variables, including the molecular weight, crosslink density, mechanical deformation, plasticizer content, and blend composition.[36–38] An unusual compositional variation of miscible polymer blends with a strong specific interaction has been shown for T_g. Painter et al.[39] proposed a modified classical thermodynamic theory to explain such behavior around T_g with numerous compositions.

Above the melt, straight lines in the retention diagrams were observed because of the establishment of the equilibrium between the solutes and the blend, an indication that the blend was in an amorphous state. All thermodynamic parameters were calculated with this zone. The slope of these straight lines can be useful for the calculation of ΔH_1^s according to eq. (7). Below T_m, all blends were mixtures of crystalline and amorphous phases. Most isotherms could not clearly identify T_g because of the kinetic effect of the diffusion

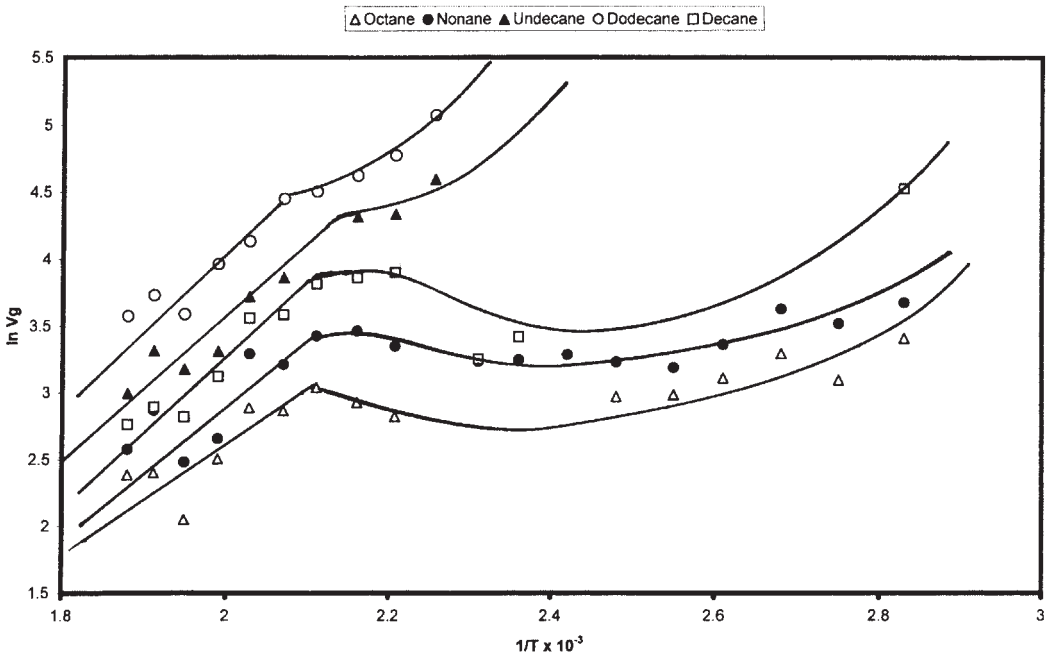

Figure 6 Retention diagram: a blend of the 75/25% AP–alkane system at 80–260°C.

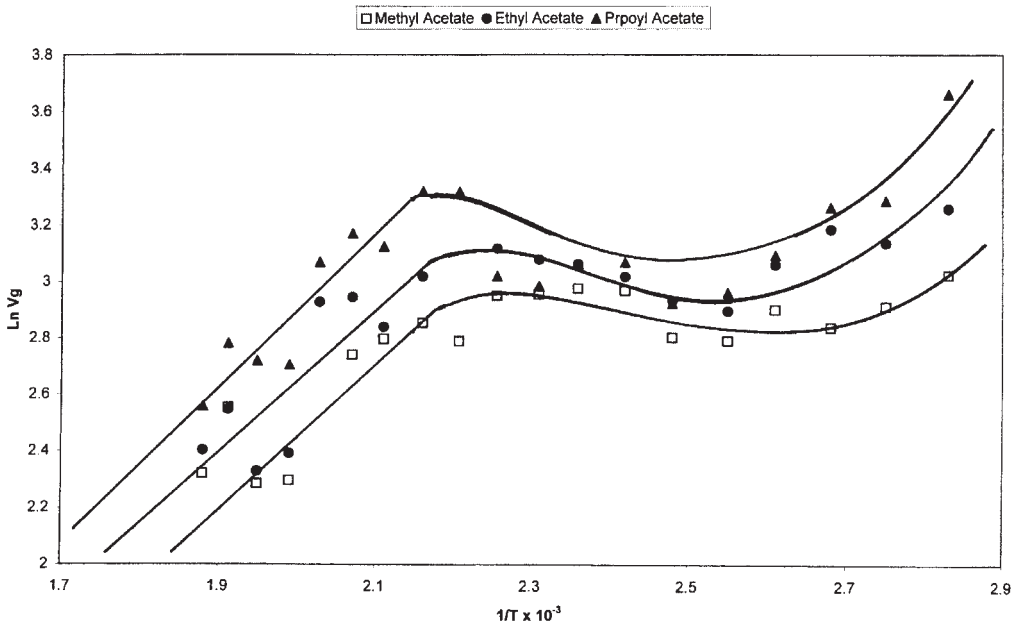

Figure 7 Retention diagram: a blend of the 75/25% AP–acetate system at 80–260°C.

of gases into the crystalline layer, and the thermodynamic calculations were not valid in this zone. When the solutes were changed from alkanes to more interactive solutes such as alcohols and diethyl amine, T_m and T_g slightly shifted from one solute to another. This effect was due to the chemical nature of the solutes, which probed the dispersive, dipole, and hydrogen-bonding interaction forces. Diethyl amine and formic acid probed the acid–base character of the blends. Water probed the wettability of the blends. Because of strong interactions of alcohols with 50/50 and 75/25 blends, retention diagrams could not be completed at higher temperatures. Alcohols as well as formic acid, diethyl amine, and water did not exit the column in a period of 20 min. This can be explained by the strong interactions of these probes with the polymer surface filled with active interaction sites such as hydroxyl groups. High retention volumes of water were observed; this was an indication of the strong interaction (hydrogen bonding), as expected, of water with the blend surface.

χ_{23}

χ_{23} was calculated with IGC and eq. (6) over a temperature range of 80–160°C. χ_{23} revealed partially negative values over a range of weight fractions (0–100% AP). Only alkanes and alcohols were used for χ_{23} calculations; other solutes could not be used because of the lack of Antoine constants in the literature. Tables II and III show the values of χ_{23} of three blends with compositions of 25/75%, 50/50%, and 75/25% AP–PCL. The negative values varied with the weight fraction from close to zero to −1.42. The lowest value was obtained with the 25/75% AP–PCL composition, and this reflected the compatibility of AP and PCL at this composition and in the temperature range of 80–160°C. χ_{23} values did not show any trend with temperature, however; it was close to zero for some solutes such as butanol. An inspection of Tables II and III confirmed our previous observation:[25] the χ_{23} values depended on the chemical nature of the solutes. However, the values did not grossly differ from one an-

TABLE II
χ_{23} of 50/50% AP–PCL Blends

Solute	80°C	90°C	100°C	110°C	120°C	130°C	140°C	150°C	160°C	25/75% 160°C
Hexane	−0.31	−0.29	−0.25	−0.33	−0.14	−0.22	−0.14	−1.23	−1.37	−0.15
Heptane	−0.18	−0.18	−0.20	−0.21	−0.14	−0.21	−0.14	−0.80	—	—
Methanol	−0.29	−0.29	−0.29	−0.19	−0.29	−0.24	−0.22	−0.22	−0.18	−1.42
Ethanol	—	−0.13	−0.15	−0.14	−0.15	−0.19	−0.17	−0.80	−0.16	−1.34
Propanol	−0.12	−0.12	−0.14	−0.13	−0.16	−0.19	−0.19	−0.16	−0.15	−1.33
Butanol	0.05	0.01	−0.03	−0.04	−0.06	−0.13	−0.15	−0.17	−0.17	−1.39

TABLE III
χ_{23} of 75/25% AP–PCL Blends

Solute	80°C	90°C	100°C	110°C	120°C	130°C	140°C	150°C	160°C
Hexane	−0.36	−0.25	−0.30	−0.13	−0.14	−0.20	−0.10	−0.04	0.06
Heptane	−0.26	−0.15	−0.28	−0.28	−0.15	−0.19	−0.06	−0.05	—
Methanol	−0.33	−0.35	−0.34	−0.24	−0.35	−0.26	−0.20	−0.20	−0.17
Ethanol	—	−0.21	−0.21	−0.24	−0.19	−0.17	−0.12	−0.12	−0.13
Propanol	−0.21	−0.19	−0.20	−0.18	−0.12	−0.12	−0.06	−0.07	−0.08
Butanol	−0.26	−0.30	−0.18	−0.15	−0.25	−0.25	−0.22	−0.19	−0.02

other except for 25/75%. Similar observations were made by several IGC researchers in the past, and they were attributed to the deficiency of the Flory–Huggins theory. Prolongo et al.[40] reported that the equation of state does not yield the true polymer–polymer parameters for polymer blend systems. They developed a method that took into account several types of interactions, such as dispersive forces, dipole–dipole interactions, and hydrogen bonding, to obtain polymer–polymer parameters independent of the chemical nature of the solute. The reported results were in agreement with those obtained from other methods used for polymer characterization. Shi and Schreiber[41] also reported a corrective measure to treat the dependence of χ_{23} on the chemical nature of the solutes. They reviewed several experimental results reported from various independent sources that suggested that surface and bulk compositions in multicomponent polymer systems (blends) generally differ and that the partitioning of vapor-phase molecules between the components of the surface layer of a solid is likely to be nonrandom. They suggested and tested experimentally a procedure with IGC for establishing the true surface composition for a polymer blend system. They found that the surface concentration of one polymer in the blend always exceeded the bulk composition (weight percentage ratio) and that the difference varied strongly with the choice of the vapor solute used. The proposed causes for this effect include the preferential adsorption of the host polymer on the chromatographic support and the migration of the additive (diluent) polymer to the surface of the stationary phase. Munk et al.[42] were the third group that developed a theory based on intermolecular interactions such as dispersive forces, dipole–dipole interactions, and hydrogen bonding to predict the miscibility of polymer pairs from the multidimensional solubility parameters of the individual polymers. Their theory allowed the evaluation of χ_{23} independently of the chemical nature of the solutes. The fourth group was Prolongo et al.,[43] who addressed the dependence of χ_{23} on the chemical nature of the solute with the Scott–Flory–Huggins theory for calculations of the interaction parameters of poly(vinyl acetate)–poly(4-hydroxystyrene). Their results indicated that the interaction parameters did show a dependence on the chemical nature of the solutes, in contrast to that predicted by the Scott–Flory–Huggins theory. They attributed the weakness of the Scott–Flory–Huggins theory to the fact that this theory assumes that the Gibbs mixing function for the ternary polymer–polymer–solute system is additive with respect to the binary contributions. They adopted the theory of Prolongo et al.[40] and recalculated the interaction parameters, obtaining negative values of χ_{23}. The recalculation confirmed the miscibility of this blend through hydrogen-bond interactions. The solute dependence was not eliminated but minimized, and only a slight variation in the χ_{23} values with the blend composition was found. On account of the uncertainty of the correction procedures used by these groups, we did not attempt to use their methods because the data cited in Tables II and III are sufficient to draw a conclusion regarding the compatibility of AP and PCL.

Crystallinity

The degree of crystallinity (X_c) of three AP–PCL blends in the temperature range of 80–220°C was achieved by the extrapolation of the linear portion of the retention diagrams (Figs. 1–7) to the crystalline region. Two retention volumes were measured: $V_{g,\text{sample}}$ is the retention volume of the solute along the curvature line in the crystalline region, and $V_{g,\text{amorphous}}$ is the retention volume of the solute along the extrapolated line of the amorphous region. With the following relationship, X_c can be assessed:

$$X_c(\%) = 100\left[1 - \left(\frac{V_{g,\text{sample}}}{V_{g,\text{amorphus}}}\right)\right] \qquad (11)$$

With eq. (11), X_c of the three blends was compared with that of pure AP. At 80°C, X_c of the three blends approached AP's X_c, which was on average 85%, except for the 25/75% blend, which showed a significant reduction. A significant reduction in X_c was shown when corn starch was blended with ethylene-*co*-vinyl acetates.[44] The X_c values observed for the 50/50% and 75/25% AP–PCL blends did not show any reduction in comparison with that of pure AP. This observation was unusual, causing an elevation in the T_m and T_g values. IGC agreed with the XRD measurements with

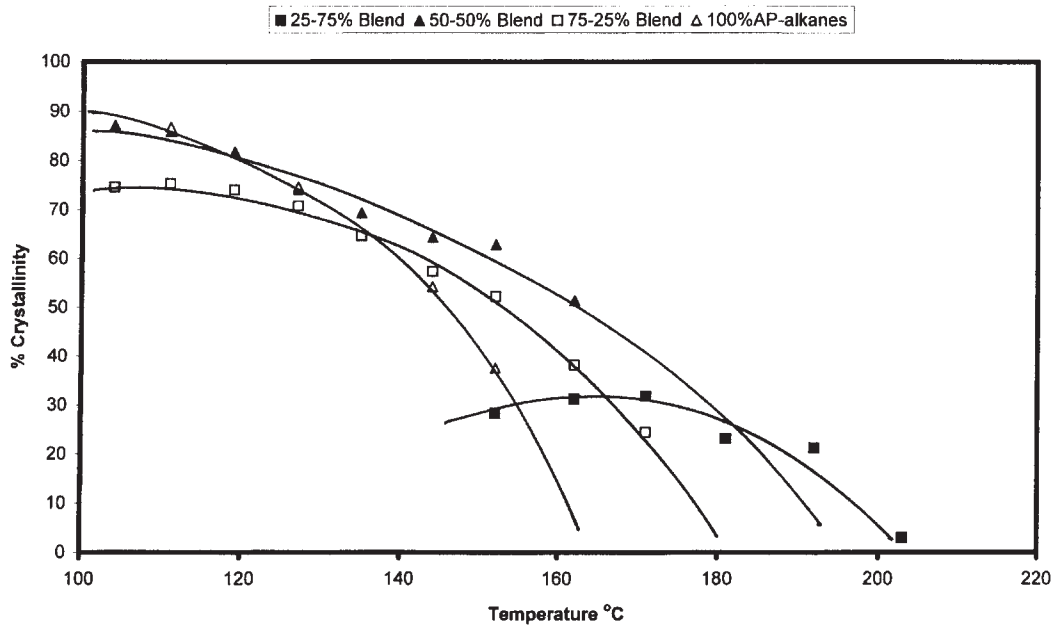

Figure 8 X_c of AP and its blends (0–100% AP) at 105–210°C.

respect to the X_c, T_m, and T_g values of the blends (see the next section on XRD experiments). As the temperature increased, X_c of the three blends and pure AP decreased as expected because of the increase in the thermal expansion of the surface. Figure 8 can be used to easily determine T_m of these blends, which is the intersection of the curve with the X axis. The curve of pure AP showed a T_m value of 166°C, which was in line with that measured by the retention diagrams and the DSC method. However, the three blends showed T_m's higher than that of pure AP, ranging from 180 to 210°C. This kind of elevation in T_m was unexpected and could be explained by the fact that other variables, such as the type of interaction that developed between the two polymers, were involved. Figure 8 shows the versatility of the IGC method by the determination of X_c at any single temperature below the T_m value, unlike the DSC method, which only provided a range of X_c values.

For polymer blends containing complex mixtures such as AP and semicrystalline homopolymers, the morphology of the blend will be more complex than that of the amorphous–amorphous polymer pair. In this case, it is possible to obtain χ_{23} and the interaction energy parameter (B_{23}) experimentally by the measurement of the T_m depression (or elevation) of a polymer mixture (blend). In the past,[23] we related the depression in T_m of a poly(vinylidene fluoride) poly(ethyl methacrylate) (PVF2–PEMA) blend to the polymer blend miscibility. Equation (12) is usually used for the calculation of the T_m depression:

$$\frac{1}{T_m} - \frac{1}{T_m{}^0} = -R\left(\frac{V_{2u}}{\Delta H_{2u}}\right) \times \left[\rho_2 \ln\left(\frac{\nu_2}{M_2}\right) + \left(\frac{\rho_2}{M_2} - \frac{\rho_3}{M_3}\right)\nu_3 + \left(\frac{B_{23}}{RT_m}\right)\nu_3{}^2\right] \quad (12)$$

where subscripts 2 and 3 refer to AP and PCL, respectively. T_m and $T_m{}^0$ are the melting point of AP in the mixture and the equilibrium melting point of pure AP (166°C), respectively. The quantities ν_2, ν_3, ρ_2, ρ_3, M_2, and M_3 are the volume fractions, densities, and molecular weights of AP and the diluent amorphous polymer, PCL, respectively, in the blend. The quantity $\Delta H_{2u}/V_{2u}$ is the heat of fusion of AP (u being the symbol for fusion). It was taken from ref. 45 as 35.90 cal/g or 45.23 cal/mL.

The first two terms in eq. (12) are the entropic contribution, and the third term is the enthalpic contribution. Because the molecular weights of both AP and PCL are greater than 80,000 g/mol, the entropic contribution is envisioned to play a minor role in the T_m depression. Therefore, the values of the first two terms will be very small and can be neglected. Then, eq. (12) reads as follows:

$$\frac{1}{T_m} - \frac{1}{T_m{}^0} = -\left(\frac{V_{2u}}{\Delta H_{2u}}\right)\left(\frac{B_{23}}{T_m}\right)\nu_3{}^2 \quad (13)$$

Equation (13) can be rewritten in this form:

$$\Delta T_m = T_m{}^0 - T_m = -T_m{}^0\left(\frac{V_{2u}}{\Delta H_{2u}}\right)B_{23}\nu_3{}^2 \quad (14)$$

where ΔT_m is the depression in the melting point of AP in the blend. Because we observed an elevation in T_m of AP in the mixture, a reversal of eq. (14) would fit the elevation trend in T_m. Multiplying eq. (14) by a negative sign yields eq. (15), which is used for the elevation in T_m in our case:

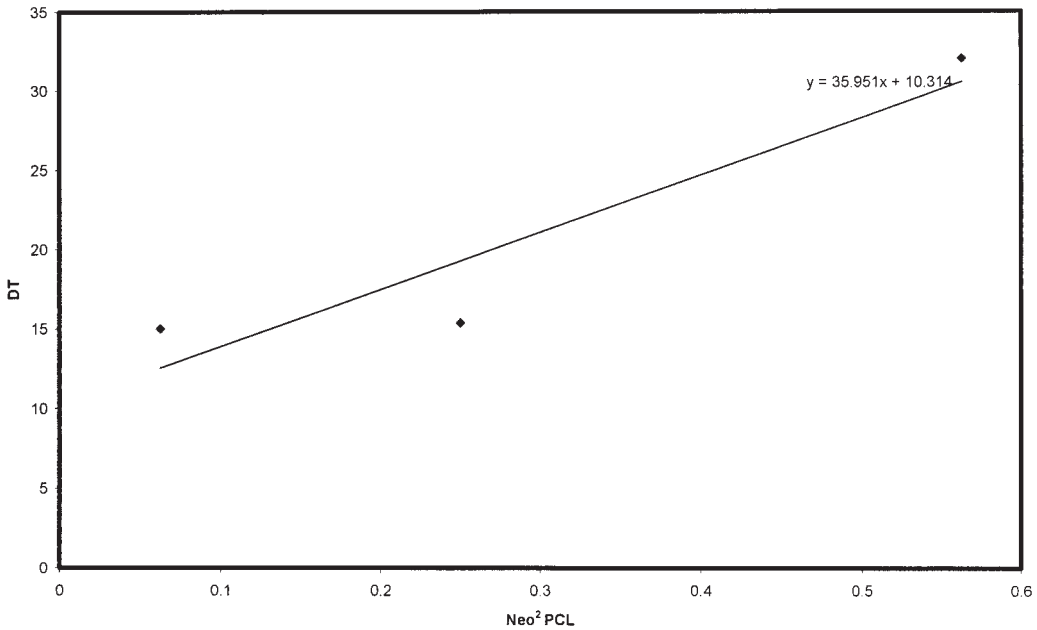

Figure 9 Elevation in T_m (DT) for AP–PCL blends.

$$\Delta T_m = T_m - T_m{}^0 = T_m{}^0\left(\frac{V_{2u}}{\Delta H_{2u}}\right)B_{23}\nu_3{}^2 \qquad (15)$$

B_{23}, as previously defined, is related to the Flory–Huggins interaction parameter χ_{23} as in the following equation:

$$B_{23} = RT_m{}^0\left(\frac{\chi_{23}}{V_3}\right) \qquad (16)$$

where V_3 is the molar volume of the diluent polymer. A plot of ΔT_m versus the volume fraction of PCL (ν_3^2) yielded a straight line (Fig. 9). The slope of the line yielded a value of B_{23} of +9.84 cal/mL and an intercept of +10.31°C. This intercept can be attributed to an entropic contribution to the mixing process. Thus, we can conclude that the mixing of AP and PCL was driven by enthalpic and entropic effects and the first two terms in eq. (12) had a role in the mixing process. The values of B_{23} and the intercept suggested the incompatibility of AP and PCL. These values explained the fact that the χ_{23} values were partially exothermic; the values were close to zero, except for the 25/75% AP–PCL composition. The 25/75% AP–PCL point in Figure 9 is actually problematic; indeed, it is driving the intercept to a higher value. Thus, the entropy of mixing plays a major role in the mixing of AP and PCL because of the large molecular weight of AP (6,600,000 g/mol). Similar observations were reported for a blend of thermoplastic starch and PCL; the thermal, thermomechanical, and mechanical characteristics of the blend clearly indicated a phase separation, as is generally found in nonmiscible polymer blends.[31] χ [eq. (16)] is considered an empirical quantity that is fit to experimental data, yet it contains substantial entropic contributions and often strongly depends on the composition.[46] The observed composition dependence shows a great richness that is yet to be understood on the basis of molecular theory that would enable the establishment of correlations between the molecular structure and interactions, on the one hand, and measured properties of χ, on the other hand. Thus, the less exothermic values of χ_{23} and the endothermic value of B_{23} suggest that both AP and PCL are partially miscible. The difference in the molar masses of AP and PCL is huge. Thus, there are differences in the chain lengths, which may cause a difference in the entropy between the two polymers. PCL may cover only several lattice sites of AP and interact through the segments on AP's surface. It is apparent that the mixing process of AP and PCL is significantly molecular-weight-dependent. The sizes and shapes of the two polymers may generate a small ratio of molecular volumes that affect the free volume variation with the blending of the two polymers, which may cause an entropy contribution to the mixing process.[47] The entropic effect on the mixing process may explain the observed elevation in the T_m and T_g values of the blend. This implies a change in the entropy of mixing at the glass transition of the blend in relation to the changes in the heat capacities of the blend at T_g. Chang et al.[48] showed that when phenolic blends were used with different polymeric modifiers, there was a higher T_g value due to the presence of extremely high OH group density and the formation of a high density of the intra-associated hydrogen bonds. The T_g deviation

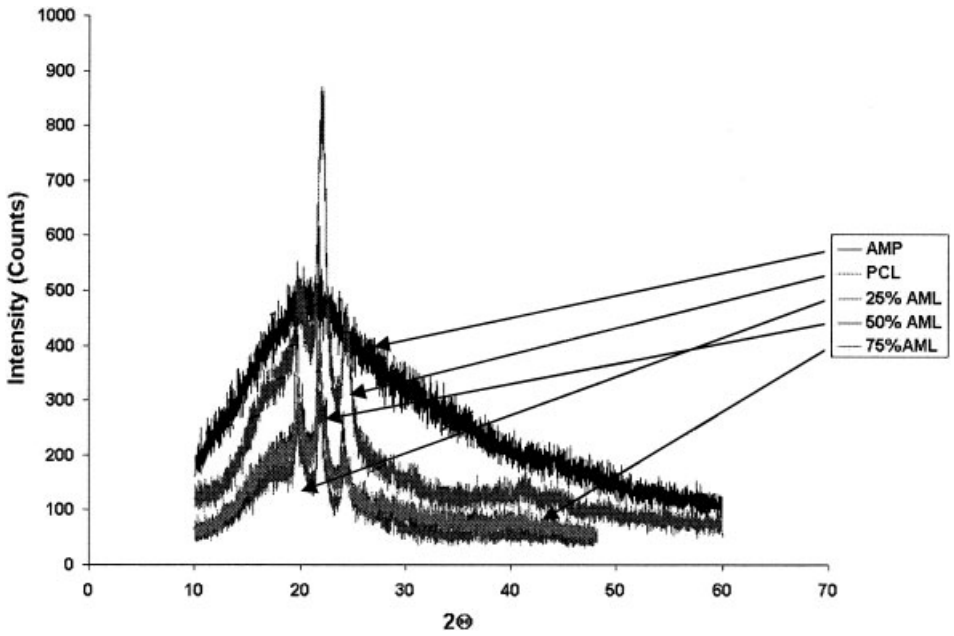

Figure 10 XRD spectra of AP, PCL, and AP–PCL blends.

is a result of entropy change corresponding to the change in the number of hydrogen-bonding interactions within these phenolic blends.

XRD analysis

XRD was used to characterize five samples with a Scitag PAD V X-ray diffractometer. Two of these samples were pure AP and PCL; the other three were 25/75%, 50/50%, and 75/25% AP–PCL blends. XRD analyses were performed by the U.S. Department of Agriculture Forest Service. Figure 10 shows the XRD analysis of these five samples, whereas Figure 11 confirms the composition of AP in the blend with the peak height (counts) at $2\Theta = 22°$. As mentioned in the previous sections, unusual behavior in the X_c, T_m, and T_g values were observed. XRD analysis agreed with the IGC analysis of these observations. XRD gives very distinct patterns for crystalline and amorphous materials. The diffracting X-rays interact with the variation

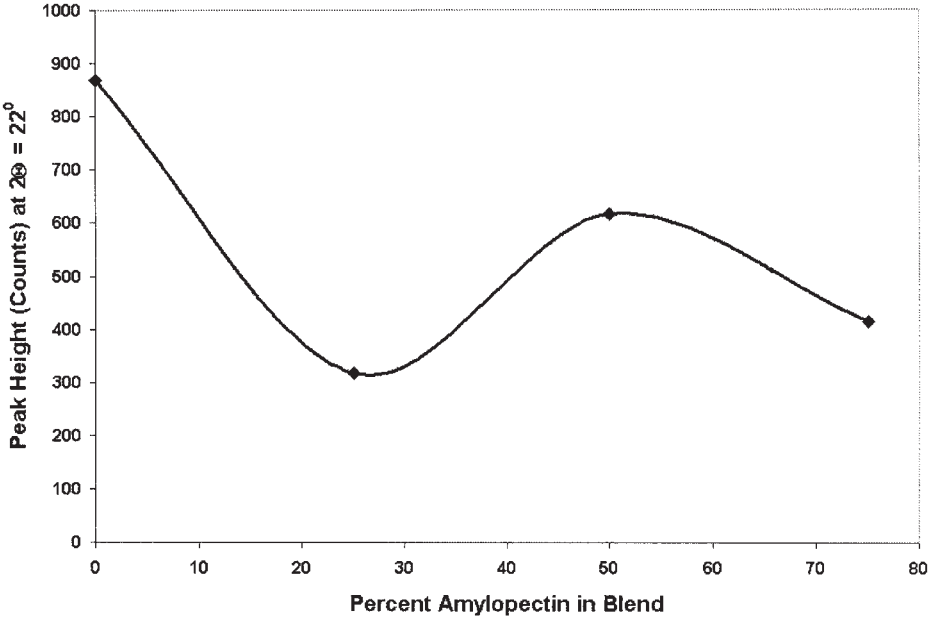

Figure 11 Peak height (counts) at $2\Theta = 22°$ versus the AP percentage in an AP–PCL blend.

of the electron density inside a sample. For a crystalline material, the periodic repeating electron density will give rise to well-defined diffraction peaks, whose widths are determined by the crystalline quality. High-quality crystalline material will give rise to sharp peaks, whose widths are limited by the instrumental resolution, whereas poor-quality crystalline material will give rise to broader, more diffuse diffraction peaks. Figure 10 shows different XRD diagrams recorded for the blend samples. The blends prepared with PCL exhibited distinct diffraction peaks, whereas pure AP did not. These patterns support our observation that PCL, when blended with AP, contributes to a crystalline character increase. Therefore, IGC is able to provide information on the crystalline characteristics of polymeric materials, which have always been of great importance for the understanding of polymer properties. Increasing the crystalline character in the blend and then extending the periodically organized area in the polymer must decrease the degree of freedom. T_m and T_g must increase (elevated). Both the IGC and XRD methods agreed on the elevation of both T_m and T_g when AP and PCL were blended. Indeed, all blends exhibited XRD peaks, whereas the reference (AP) did not. Figure 10 shows that all the AP–PCL blends had elevated T_m and T_g values.

Surface energy

The dispersive component of the surface energy of AP and three AP–PCL blends was calculated with only the alkane series in the temperature range of 80–200°C. According to eq. (5), plots of $RT \ln V_g^0$ (kJ/mol) versus the number of carbons in the alkane series were generated for each temperature. Linear relationships were obtained in all these plots, and the slope of the straight lines was computed as ΔG_a^{CH2}. With eq. (6), γ_s^d of the AP–PCL blends was calculated as a function of temperature. The cross-sectional area[20] of an adsorbed CH_2 group (a_{CH_2}) was estimated to be 6 Å^2. The surface-free energy of a solid containing only CH_2 groups (γ_{CH_2}) was computed as a function of temperature as follows:

$$\gamma_{CH_2} = 36.80 - 0.058t \qquad (17)$$

where t is the temperature (°C).

Table IV shows a comparison of the γ_s^d values of the pure AP and three blends at 150°C. The γ_s^d values ranged from 16.09 mJ/m^2 for pure AP to 38.26 for the 50/50% AP–PCL blend. The low value of γ_s^d for pure AP was expected because the AP surface was still crystalline at 150°C and was mechanically weak. An increase in the temperature lowered the values of γ_s^d of pure AP and the three blends, as expected, and this may have been caused by the expansion of the surface above the melt. The surface energy was doubled when the composition of the blend was 50/50%. At a composition of 25/75%, the γ_s^d value was slightly increased. This slight increase in the γ_s^d values revealed the contribution of PCL to the surface energy upon mixing. However, when the composition of the blend was mostly AP (75/25%), γ_s^d was considerably decreased, in contrast to that of the 25/75% composition.

TABLE IV
γ_s^d of Pure AP and Its Blends at 150°C

AP–PCL blend	γ_s^d (mJ/m^2)
100% AP	16.09
25/75%	18.55
50/50%	38.26
75/25%	6.5

CONCLUSIONS

IGC complemented the DSC method in obtaining T_g (105°C) and T_m (160–166°C) of a starch-based polymer, AP, with a molecular weight of 6,000,000 g/mol. IGC was superior to DSC when X_c and γ_s^d were obtained. IGC was able to measure X_c at a single temperature and provide a range of crystallinities below AP's T_m. IGC found that AP is crystalline at room temperature and melts at 160°C. X_c of AP was important in explaining the low values of the surface energy found by IGC. IGC was also able to measure the interaction parameters of a variety of alkanes with AP in a wide temperature range, yet it determined the solubility of the blends in these solutes. It was also able to determine the blend compatibility over a wide range of temperatures and weight fractions. The χ_{23} and B_{23} parameters agreed well on the partial miscibility of the two polymers. It was also capable of measuring the wettability of AP as well as the acid–base interactions of ethyl amine and formic acid with AP.

The authors thank Mandla A. Tshabalala of the U.S. Department of Agriculture Forest Service (Madison, WI) for performing thermal analysis on amylopectin with the differential scanning calorimetry method and X-ray diffraction measurements on amylopectin–poly(ε-caprolactone) blends. Thanks are also due to Souad Ammar (Interfaces, Traitements, Organisation et Dynamique des Systèmes, Équipe Chimie des Matériaux Divisés et Catalyse, Université Paris 7).

References

1. Holmes, P. A. In Developments in Crystalline Polymers; Bassett, D. C., Ed.; Elsevier: London, 1988; Vol. 2, p 1.
2. Doi, Y. Microbial Polyesters; VCH: New York, 1990.
3. Holmes, P. A. Phys Technol 1985, 16, 32.

4. Barham, P. J.; Keller, A. A. J Polym Sci Part B: Polym Phys 1986, 24, 69.
5. Zhang, L.; Deng, X.; Zhao, S.; Huang, Z. Polym Int 1997, 44, 104.
6. Fanta, G. F.; Swanson, C. L.; Doane, W. M. J Appl Polym Sci 1990, 40, 811.
7. Shogren, R. L.; Thompson, A. R. J Appl Polym Sci 1992, 4, 1971.
8. Shogren, R. L.; Greene, R. V.; Wu, Y. V. J Appl Polym Sci 1991, 42, 1701.
9. Alghamdi, A.; Melibari, M.; Al-Saigh, Z. Y. J Polym Environ 2005, 13, 319.
10. Chiellini, E.; Solaro, R. Adv Mater 1996, 8, 305.
11. Amass, W.; Amass, A.; Tighe, B. Polym Int 1998, 47, 89.
12. Fringant, C.; Desbrieres, J.; Rindaudo, M. Polymer 1996, 37, 2663.
13. Al-Saigh, Z. Y.; Guillet, J. In Encyclopedia of Analytical Chemistry: Instrumentation and Applications; Meyers, R., Ed.; Wiley: Chichester, England, 2000; Vol. 9, p 7759.
14. Al-Saigh, Z. Y. Polym Int 1996, 40, 25.
15. Al-Saigh, Z. Y. Polymer 1999, 40, 3479.
16. Chehimi, M. M.; Pigois-Landureau, E.; Delamar, M. M. J Chim Phys 1992, 89, 1173.
17. Landureau, E.; Chehimi, M. M. J Appl Polym Sci 1993, 49, 183.
18. Chehimi, M. M.; Abel, M. L.; Perruchot, C.; Delamar, M.; Lascelles, S. F.; Armes, S. P. Synth Met 1999, 104, 51.
19. Papirer, E.; Eckhardt, A.; Muller, F.; Yvon, J. J Mater Sci 1990, 25, 5109.
20. Papirer, E.; Ligner, G.; Vidal, A.; Balard, H.; Mauss, F. In Chemically Modified Oxide Surfaces; Leyden, E.; Collins, W. T., Eds.; Gordon & Breach: New York, 1990; p 361.
21. Papirer, E.; Balard, H.; Vidal, A. Eur Polym J 1988, 24, 783.
22. Papirer, E.; Roland, P.; Nardin, M.; Balard, H. J Colloid Interface Sci 1986, 113, 62.
23. Al-Saigh, Z. Y.; Chen, P. Macromolecules 1991, 24, 3788.
24. Al-Gahmdi, A.; Al-Saigh, Z. Y. J Polym Sci Part B: Polym Phys 2000, 38, 1155.
25. Al-Saigh, Z. Y.; Munk, P. Macromolecules 1984, 17, 803.
26. Al-Saigh, Z. Y. Int J Polym Characterization Anal 1997, 3, 249.
27. Papirer, E.; Brendle, E.; Ballard, H.; Vergelati, C. J Adhes Sci Technol 2000, 14, 321.
28. Tshabalala, M. A.; Denes, A. R.; Williams, R. S. J Appl Polym Sci 1999, 73, 399.
29. Tshabalala, M. A. J Appl Polym Sci 1997, 65, 1013.
30. Bastioli, C.; Cerrutti, A.; Guanella, L.; Romano, G. C.; Tosin, M. J Environ Polym Degrad 1995, 3, 81.
31. Averous, L.; Moro, L.; Dole, P.; Fringant, C. Polymer 2000, 41, 4157.
32. Flory, P. J. Principles of Polymer Chemistry; Cornell University Press: Ithaca, NY, 1953.
33. Sanches, I. Annu Rev Mater Sci 1983, 13, 387.
34. Fowkes, F. W. Ind Eng Chem 1964, 561, 40.
35. Fowkes, F. W. Ind Eng Chem Prod Res Dev 1967, 56, 40.
36. Card, T. W.; Al-Saigh, Z. Y.; Munk, P. J Chromatogr 1984, 301, 261.
37. Gibbs, J. H.; DiMarzio, E. A. J Chem Phys 1958, 28, 373.
38. Gibbs, J. H.; DiMarzio, E. A. J Chem Phys 1958, 28, 807.
39. Coleman, M. M.; Xu, Y.; Painter, P. C. Macromolecules 1994, 27, 127.
40. Prolongo, M. G.; Masegosa, R. M.; Horta, A. Macromolecules 1989, 22, 4346.
41. Shi, Z. H.; Schreiber, H. P. Macromolecules 1991, 24, 3522.
42. Munk, P.; Hattam, P.; Abdual-Azim, A.; Du, Q. Makromol Chem Macromol Symp 1990, 38, 205.
43. Lezcano, E. G.; Coll, S. C.; Prolongo, M. G. Macromolecules 1992, 25, 6849.
44. Ramkumear, D. H. S.; Bhattachrya, M. J Mater Sci 1997, 23, 2565.
45. Ramkumear, D. H. S.; Yang, Z.; Bhattachrya, M. Polym Network Blends 1997, 7, 31.
46. (a) Masegasa, R. M.; Prolongo, M. G.; Hirota, A. Macromolecules 1986, 19, 1478; (b) Murray, C. T.; Gilmer, J. W.; Stien, R. S. Macromolecules 1985, 18, 996.
47. Adsriana, I. P.; Freed, K. F. J Chem Phys 1989, 90, 2017.
48. Wu, H. D.; Chu, P. P.; Ma, C. M.; Chang, F. C. Macromolecules 1999, 32, 3097.